Supporting Information of "Complex-amplitude Hologram by Ultra-thin Dielectric Metasurface"

Qiang Jiang,*[a] Liangcai Cao,[b] Lingling Huang,[a] Zehao He[b] and Guofan Jin [b]

[1]School of Optics and Photonics, Beijing Institute of Technology, Beijing 100081, China;
[2] State Key Laboratory of Precision Measurement Technology and Instruments, Department of Precision Instruments, Tsinghua University, Beijing 10084, China

1. Point Source Algorithm and Angular Spectrum Method

1.1 Point source algorithm

The complex-amplitude CGH and the phase-only CGH are generated by point source algorithm. Random phase is eliminated when calculating the complex-amplitude CGH, while it is adopted when calculating the phase-only CGH. As is shown in Figure S1, in the point-based approach, the 3D scene is represented as aggregated point sources. Assuming that the coordinates of points on the CGH plane are (x, y, z) and the coordinates of points representing the object are (x_m, y_m, z_m), the distance r_m between points on the object and points on the CGH plane can be expressed as

$$r_m = \sqrt{(x_m - x)^2 + (y_m - y)^2 + (z_m - z)^2} \ .$$

Then the optical field for the entire 3D scene is simply given by

$$h(x, y) = \sum_m \frac{A_m}{r_m} \exp(-\frac{j2\pi}{\lambda} r_m)$$
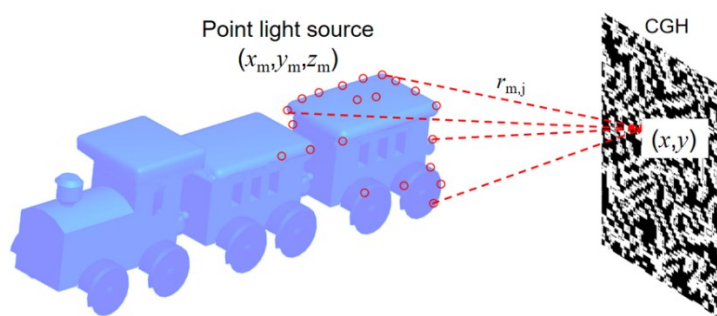
where A_m is the light intensity.

Fig. S1 Point source algorithm.

In phase-only CGH, the amplitude is discarded, leading to a reconstructed image with much high-frequency components but less low-frequency components. To improve the quality of the reconstructed image, a random phase is attached to

simulate the diffusive effect of the object surface. For complex-amplitude CGH, the complex amplitude remains the entire information and no random phase modulation is required.

1.2 Angular spectrum method

Assuming the complex field in the hologram plane is $h(x, y)$, the spatial spectrum, defined as the complex amplitude density of a plane wave component with a spatial frequency of (u, v), can be expressed as

$$H(u,v) = \int\int_{-\infty}^{\infty} h(x,y) \exp\left[-j2\pi\left(f_x x + f_y y\right)\right] dxdy$$

In this formalism, $h(x, y)$ is decomposed into a series of 3D plane waves propagating in different directions. The spatial frequency (u, v, w) determines the propagation direction of each plane wave. As shown in Figure S2, the spatial frequency can be expressed by the direction cosine (α, β, γ)

$$u = \alpha / \lambda; v = \beta / \lambda; w = \gamma / \lambda$$

$$w = \frac{1}{\lambda}\sqrt{1 - \lambda^2 u^2 - \lambda^2 v^2}$$

Since the shape of the wavefront does not change when the plane wave propagates in free space, and only a phase delay related to the propagation distance is generated. The spatial spectrum $E(u, v)$ in the image plane can be obtained from $H(u, v)$ after propagation for a distance of z,

$$E(u,v) = H(u,v) \exp\left[jkz\sqrt{1 - \lambda^2 u^2 - \lambda^2 v^2}\right]$$

Then the complex field $e(x_1, y_1)$ in the image plane can be obtained by using the inverse Fourier transform.
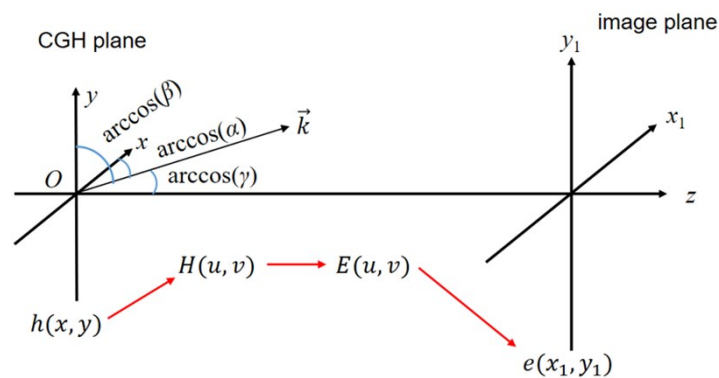

Fig. S2 Illustration of the angular spectrum theory

2. Numerical Simulation

The amplitude and phase response are analyzed using the commercial software FDTD solutions (Lumerical). Before simulation, the refractive indices of the fused silica, the silicon film and the PDMS are all experimentally measured by an ellipsometer. By independently changing the width W_1 and rotation angle θ, the amplitude and phase responses are obtained, as shown in Figure S3.
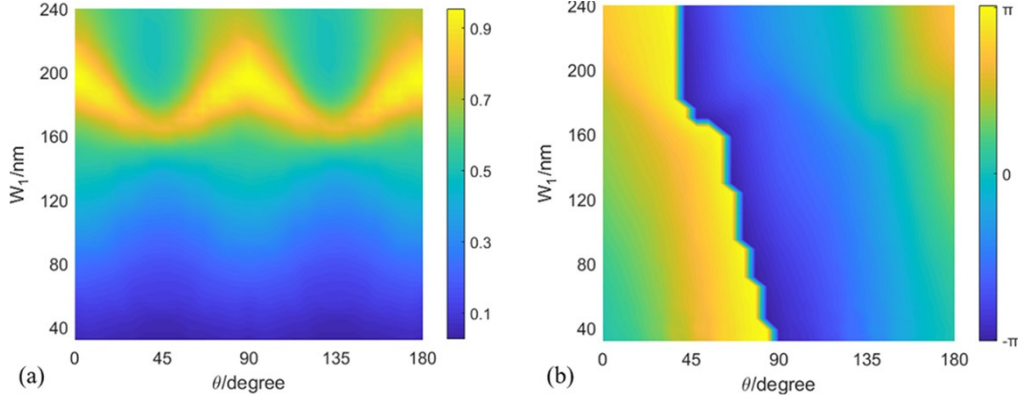

Fig. S3 Amplitude (a) and phase (b) distribution of the meta-atom when W_1 and θ change.

2. Discussion

Figure 2 shows that the polarization conversion efficiency of RCP light has two peaks in the range of 1.4-1.7 μm. The wavelength-tunable laser used in the experiment has a tunable range of 1.480-1.630 μm. When tuning the wavelength of the laser and keeping the output power unchanged, the captured image is clear in the range of 1.502-1.585 μm. This indicates that the proposed metasurface can work over a wide wavelength range. The measured power of the holographic images is shown in Figure S4. It is consistent with the theoretical analysis shown in Fig. 1d, the discrepancy is caused by the reasonable fabrication error of the metasurface.
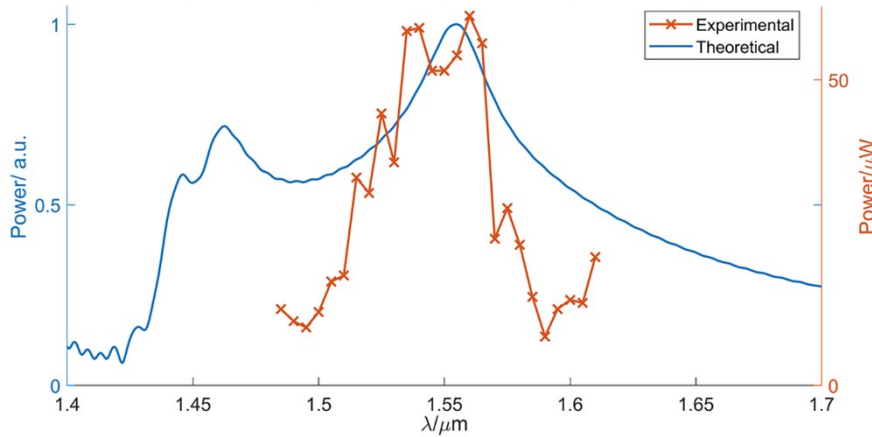

Fig. S4 Theoretical and measured power of the holographic image at different wavelengths.